Process Development and Techno-Economic Analysis for

2 Mechanochemical Recycling of Poly(ethylene terephthalate)

- 4 Elisavet Anglou[†], Arvind Ganesan[†], Yuchen Chang, Kinga M. Gołąbek, Qiang Fu, William
- 5 Bradley, Christopher W. Jones, Carsten Sievers, Sankar Nair*, and Fani Boukouvala*
- 6 School of Chemical & Biomolecular Engineering, Georgia Institute of Technology, Atlanta, GA
- 7 *30332, USA*

1

3

10

- 8 *Corresponding authors: fani.boukouvala@chbe.gatech.edu; sankar.nair@chbe.gatech.edu
- 9 [†] Authors contributed equally.
- 11 Keywords: ball milling, mechanochemical reactor, PET, techno-economics, monomers,
- separations, process flow modelling, recycling

Abstract

14

15

16

17

18

19

20

21

22

23

24

25

26

27

28

29

30

31

32

Chemical recycling of consumer plastics has garnered great attention towards achieving circular economy goals. Particularly in the case of PET waste, mechanochemical depolymerization in ball mill reactors has recently been identified as a very promising technology due to the high conversion rates achieved under mild conditions. While the absence of solvents in the reaction mixture reduces significant separation costs, mechanochemical depolymerization still presents challenges with respect to the efficient separation and purification of monomers. Thus, meticulous experiments, process modeling, and simulations are essential for demonstrating the separation and purification of monomers. In this study, we present the lab-scale separation process flow for the recovery of terephthalic acid (TPA) and ethylene glycol (EG) from mechanochemically depolymerized polyethylene terephthalate (PET). We additionally examine the use recycling of ideal PET powder and commercial samples (e.g., PET fibers, bottles, and food containers) as feedstocks. The process parameters are optimized to achieve 97%+ of monomer recovery with 99%+ purity. The complete recovery of EG, and recycling of process water enables a 'zero-liquid discharge' process design. Subsequently, we conduct a techno-economic analysis (TEA) to evaluate the economic potential of the proposed sequence, which resulted in a positive net present value (NPV) for the different scenarios and a minimum selling price (MSP) of \$0.99/kg. Finally, we compare the economic potential of mechanochemical recycling of PET to fossil-based production and other recycling methodologies based on economic metrics.

1. Introduction

33

34

35

36

37

38

39

40

41

42

43

44

45

46

47

48

49

50

51

52

Plastics have revolutionized our daily lives due to their chemical stability, durability, and low cost, gradually replacing other materials such as glass, steel, or wood across a wide range of applications [1,2]. However, a significant amount of these plastics ends up in landfills and marine environments [3–5]. As of 2018, the global production of plastic reached 359 million tons [6], with only 10% of this volume being recycled and just 2% being processed through closed-loop recycling [7], while 79% was left to accumulate in landfills or the natural environment [1]. Geyer et al. [1] project the annual production of plastics to reach 1.1 billion tons by 2050. In addition to interference in natural habitats [8,9], the breakdown of plastics into microplastics [10] and toxic water-soluble chemicals [11] has garnered increasing attention in the context of their environmental and economic implications. Thus, the effective management of plastic waste and their end-of-life treatment have garnered great attention. Specifically, there is a growing interest in transitioning to a circular economy (CE) in which plastics will be efficiently and sustainably recycled back into the economy. Poly(ethylene terephthalate) (PET) amounted to over 32 million metric tons of global annual plastic production in 2019 [12]. PET is made by co-polymerization of terephthalic acid (TPA) and ethylene glycol (EG) via esterification, and is widely used to make beverage bottles, packaging, carpets, and clothing. Currently, processing of PET waste through mechanical recycling is the most widely implemented technology [13–16]. However, mechanical recycling usually leads to degradation of the functional properties of PET waste due to the mechanical and thermal stresses/breakdown acting on the polymer during reprocessing [2,7,17]. Consequently, PET can

53 be mechanically recycled only a limited number of times and only if mixed with large quantities 54 of virgin polymers [18,19]. 55 Alternatively, the relative ease of cleaving an ester bond (C-O), as compared to C-C bonds in other 56 polymers, has generated greater interest in the chemical recycling of PET into monomers [2,17]. 57 Chemical recycling, although less common, has emerged as a promising alternative to traditional 58 recycling methods. Polymers are directly converted to monomers or oligomers that may be further 59 purified to the same molecules as virgin materials, thus avoiding degradation of physical and 60 chemical properties, and stepping towards a circular plastics sector with lower dependence on 61 petrochemical feedstock [2,20–23]. Solvent-assisted chemical breakdown of PET (solvolysis) has 62 made large progress over the last decade [2,22]. Hydrolysis of PET in acidic [24–26], basic [27– 63 30], and neutral [31,32] conditions are widely studied. Glycolysis [33–35] and (more generally) 64 alcoholysis [36–38] are also explored for homogeneous depolymerization of PET. Typically, these 65 conventional processes operate at high temperatures (100-300°C) and pressures (up to 20 bar) with 66 high solvent-to-PET ratios (from 5 to 20), driving up the depolymerization and separation costs. 67 In contrast, the advent of mechanochemical depolymerization creates a potential paradigm change 68 [19,39,40]. The depolymerization reaction is performed in a ball mill, while the energy necessary 69 to drive the reaction is supplied to the system through the impacts of the balls with solid particles 70 [2]. This approach has distinct advantages: (a) it does not require a reaction solvent nor extreme 71 operating conditions, and (b) the ball mill uses electrical energy input rather than process heating. 72 Mechanochemical routes has been recently demonstrated for the depolymerization of various types 73 of plastics including PET, PS, PVC and others [41–47]. The conversion of plastics into valueadded products are exciting alternatives [45,46]. Specifically for the case of PET, Strukil et al. [39] recently reported a high conversion of PET to monomers via milling. Tricker et al. [19] demonstrated complete depolymerization of PET and stoichiometric amounts of sodium hydroxide (NaOH) to ethylene glycol (EG) and disodium terephthalate salt (Na₂TPA). The recycling of PET into monomers presents a unique opportunity to evolve into a circular economy. Mechanochemical PET depolymerization presents new opportunities and challenges in the development of overall processes that are economically viable. For example, the solid depolymerization products from the ball mill consist of monomers, unreacted polymers (if any), catalysts (if any), and other impurities (dyes, additives, etc.) originating from the feedstock. These pose new separation issues compared to conventional solvolysis, which generally results in a multicomponent mixture that is also prone to the formation of azeotropes. Thus far, solvolysis processes have used separation processes such as filtration (to remove unreacted polymers) and crystallization of TPA or BHET by acidification or drying [29,33,37,48]. Recently, Singh et al. [49] also addressed the large cost of separating EG from excess solvent in conventional solvolysis. Process simulators such as Aspen Plus [50] or gProms [51] are used to obtain the mass and energy flows, which then allows for the quantitative comparison of different scenarios or sequences of unit operations [52–55]. By coupling these simulation results with costing correlations or other information from manufacturers, the fixed and operating expenses can be determined. This enables the comprehensive assessment of how the design variable impact the projected economics [56– 58]. While there is a significant body of literature on PET depolymerization, only limited information is available on the techno-economic aspects of PET chemical recycling [49,56,57,59].

74

75

76

77

78

79

80

81

82

83

84

85

86

87

88

89

90

91

92

93

Particularly for the case of PET plastic waste, Singh et al. [49] applied a technoeconomic analysis (TEA) and life cycle assessment (LCA) framework to assess the social and economic implications of an enzyme-catalyzed recycling PET depolymerization process. Their analysis showed that enzymatic recycling can be potentially cost-effective relative to producing new (petro-derived) PET. The projected minimum selling price (MSP) for this method (\$1.93/kg) was found to be higher than the market averages (currently \$1.14/kg for virgin TPA), but the sensitivity analysis revealed that the MSP could drop if higher conversion rates could be achieved. Uekert et al. [58] conducted a comparative evaluation of the previously known recycling routes for PET (and other plastics) using various economic and sustainability metrics. Their findings indicate that glycolysis offers the best overall performance for PET recycling, with an MSP of \$0.96/kg (BHET) that is competitive with virgin PET. To the best of our knowledge, quantitative process and economics analysis have not been performed yet for mechanochemical or mechanocatalytic depolymerization pathways.

In this work, we combine lab-scale experimental design, validation, and a process systems engineering approach to design, simulate, and optimize an integrated process flowsheet that facilitates the mechanochemical depolymerization of PET waste to its monomeric molecules (**Fig.** 1). The primary products of the mechanochemical reaction of PET with sodium hydroxide (NaOH) are disodium terephthalate (Na₂TPA) and ethylene glycol (EG). A sequence of unit operations is designed and validated experimentally to facilitate the selective extraction, purification of individual monomers. The depolymerization of ideal (PET powder) and commercial feedstocks (textiles, PET bottles and food containers) are studied. Subsequently, the process flowsheet is modeled in the Aspen Plus using pre-defined and custom-defined unit operation models. The

flowsheet is designed for a scaled-up process, with throughput rates estimated based on total PET recycling rates in the state of Georgia, USA. Calculations of mass and energy flow are utilized to determine equipment sizing and utility requirements. A techno-economic analysis (TEA) is then conducted. These integration of all these tools and results enable the assessment of the future economic potential of the process. Through sensitivity analyses, the significance of process design variables such as reactor or separations specifications, as well as the impact of feedstock and raw material price volatility on the projected minimum selling price (MSP) is quantified.

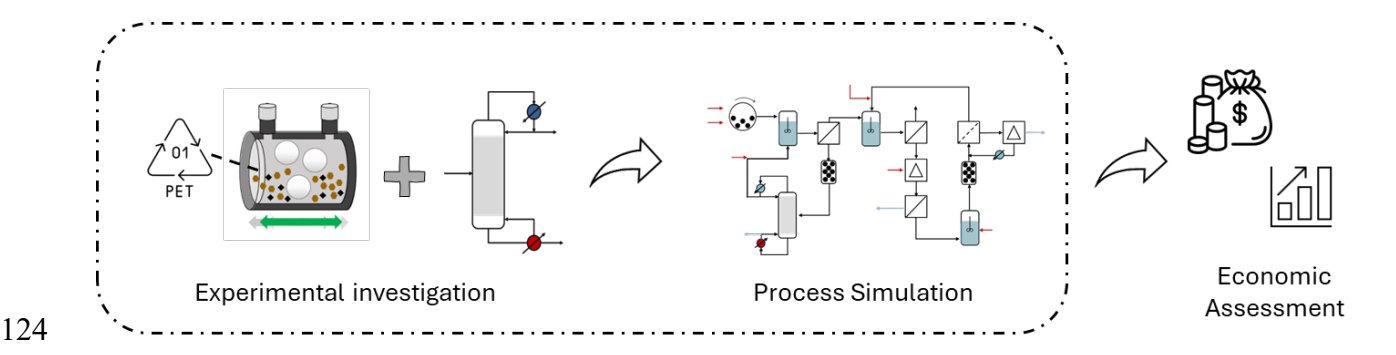


Fig. 1: Workflow of the present analysis

The rest of the paper is organized as follows. Section 2 highlights the methods used in the experimental and computational part of the work. Section 3 provides an overview of the proposed design and discusses the experimental validation, explores the techno-economics of the integrated process and presents the results of the sensitivity analyses. Finally, Section 4 summarizes the conclusions of the work and outlines future prospects.

2. Experimental and Modeling Methods

2.1.Materials

Poly (ethylene terephthalate) (PET) granules (semi-crystalline > 50%, Sigma Aldrich), commercial Kolon textiles (brown color), clear PET bottles and food containers, sulfuric acid (VWR), disodium terephthalate (Alfa Aesar), acetone (VWR), sodium sulfate (Sigma Aldrich), D₂O (Sigma Aldrich), Sodium trimethylsilylpropanesulfonate (Fischer Scientific), deuterated trifluoroacetic acid (TFA-d) (Sigma Aldrich), and sodium hydroxide (Sigma Aldrich). Deionized water from the EMD Millipore water purification system, DuPont FilmTec XC70, Whatman filter papers, and VWR 0.2 μm syringe filter were used in this work.

2.2. Composition Analyses

Solution NMR measurements were performed with Bruker Avance III 400 MHz. SEM images were obtained with Hitachi SU 8010 scanning electron microscope. Solvent recovery was performed with Buchi Rotavapor R-100. SO_4^{2-} ions are measured by IC. The ion chromatography measurements were performed with a Shimadzu HPLC system equipped with a conductivity detector (Shimadadzu, CDD-10AVP, USA). IonPac® AS11 (250 mm × 2 mm ID) was used with a column temperature of 30 °C, mobile phase of 10 mM NaOH (0.30mL/min) and injection volume is 1 μ L. SEM images of the TPA crystals were obtained with Hitachi SU 8230 scanning electron microscope.

2.3. Extraction of EG and Na₂TPA

Typically, the depolymerized mixture was dispersed in acetone (1:1 mass ratio), the mixture was stirred at 200 rpm for 5 minutes, and subsequently filtered with a 0.2 μm syringe filter. The recovery of EG from the acetone stream was performed with a rotary evaporator at 370 mbar, 50 °C. Na₂TPA was extracted by washing with water (maintain Na₂TPA under 10 wt.%). Unreacted PET (if any) was separated with a 0.2 μm PTFE filter. TPA was crystallized and precipitated by slow addition of conc. H₂SO₄ (0.5 mL/min) to the aqueous solution of Na₂TPA. TPA crystals were isolated with a 5 μm polycarbonate filter. The crystals were dried at 50 °C overnight. EG and TPA recoveries were estimated with solution NMR measurements with D₂O as the solvent.

2.4. Water Recovery

Salt rejection (Na₂SO₄) measurements on a DuPont FilmTec XC70 were performed in a Sterilitech high-pressure dead-end stirred cell (HP4750X) with 300 mL volume feed capacity. Ion rejection performances were evaluated with Ion Chromatography (IC).

2.5. Process Simulations

Ball Mill Reactor Simulation

The industrial ball milling configuration typically involves a rotating cylindrical vessel filled with SS balls and reactants (e.g, PET waste and NaOH particles). High-fidelity DEM simulations were performed in the EDEM commercial software [60] based on the operating parameters listed in **Table 1** to determine the required torque requirements. **Fig. 2** shows a visual representation of the simulation setup. The Hertz-Mindlin (no-slip) contact model was selected as it is appropriate for

spherical shapes and has been previously utilized in similar ball-milling applications. The material and contact parameters that are required as inputs to DEM simulations were taken from the available milling literature [61]. A rotating cylindrical geometry is designed for the industrial ballmill reactor. Based on the experimental findings of our previous study, the achieved monomer yield follows a linear relationship with the ball-to-powder mass ratio (BPR) parameter [19]. If the industrial-scale ball mill reactor can maintain equivalent BPR values, the number of grinding balls and the size of the reactor can be evaluated for a constant PET waste feed. Higher BPR values correspond to higher yields with full depolymerization achieved when BPR = 22.9 with a reaction time of 20 minutes. In the context of this work, a BPR of 22.9 was used to design the reactor and the operating conditions. Results from the DEM simulations are used for the evaluation of the annual electricity cost for the ball milling system. The maximum torque load requirements were extracted from the high-fidelity DEM simulation. Based on the selected operating settings, the energy consumption of the ball-mill reactor was estimated at 125 kW. The required capital expenditure is calculated using the correlations provided by Seider [62]. Our previous work provides a more detailed analysis on the selection of operating conditions that lead to 100% conversion, the evaluation of the capital expenditure of the ball-mill reactor and the estimation of the energy consumption [63].

169

170

171

172

173

174

175

176

177

178

179

180

181

182

183

184

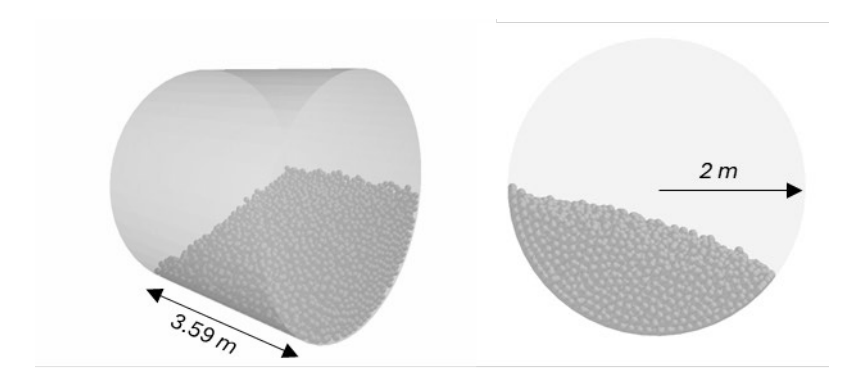


Fig. 2: The industrial ball mill reactor as designed and simulated in the EDEM software.

Table 1: Operating settings of the ball mill reactor.

Parameter	Value
Volume (m ³)	45
Number of balls	9016
r _{ball} (mm)	60
Fill-level (%)	30
Conversion	100
Ball-to-Powder ratio	22.9

The ball mill consumables include media consumption (SS balls) and play a crucial role in the grinding process. Over time, due to the wear and tear, the balls need to be replaced on a regular basis determined by the wear rate of the ball charge [64,65]. In the cement industry, the replacement period is scheduled based on a wear rate of 35 - 70 gram_{steel}/metric ton whereas for limestone grinding a wear rate of 500 gram_{steel}/metric ton is typically used [64,65]. In the context

of our application, a wear rate of 50 gram_{steel}/metric was selected as a more conservative scenario, given that the PET polymers are expected to be less hard than cement or limestone. The total steel mass is evaluated, and the replacement cost is estimated based on the all-in steel rate (US \$4300/metric ton) [65].

ASPEN flowsheet simulation of integrated process

After the integrated process (reactors, separators) was designed and demonstrated experimentally at the lab-scale, the flowsheet was modeled in Aspen Plus V12 (Aspen Technology Inc.) [50]. A processing capacity of 48 metric tons per day of PET waste was simulated, equivalent to an hourly input rate of 2,000 kg/hr. This is based on the amount of PET waste collected in the state of Georgia, USA for 2018 as reported by the National Association for Plastic Container Resources (NAPCOR) [66]. Most of the reaction components were chosen from the existing Aspen databases while those that were not available were defined based on their molecular structures and boiling points. Other physical properties were retrieved from the NIST database or estimated via Aspen Plus Properties Constant Estimation System (PCES).

The mass balances for all the purification steps were validated through experiments as described in the previous subsection. Throughout this work, it is assumed that the laboratory-scale conversions and separation efficiencies can be maintained at a larger scale. All the design parameters entered in the Aspen Plus simulation are summarized in **Table 2**. These parameters were experimentally validated at the laboratory scale (see Results and Discussion).

Table 2: Summary of the parameters and design specifications in the baseline model setup.

Unit	Block	Design variable	Baseline case
Ball mill	User-defined	Conversion	100%
Distillation column	RadFrac	Number of trays	6
Distination column	Radi iac	Reflux ratio	1.2
Acidification reactor	RStoic	Equilibrium reaction	
Neutralization reactor	RStoic	Equilibrium reaction	
Pump	Pump	Isentropic efficiency	0.8
F141	Carranatan	Solid separation	1
Filter 1	Separator	efficiency (slurry)	1
File 2	C	Solid separation	1
Filter 2 Separator		efficiency (PET)	1
Solid separation		0.00	
Filter 3	Separator	efficiency (TPA)	0.98
Corretallines	Correcte 11:	Temperature (°C)	14.4
Crystallizer	Crystallizer	Pressure (bar)	1

2.6.Economic Analysis

Operating (e.g., raw material, utility costs) and capital (equipment sizing) expenditures were estimated based on the material and energy balance results from the Aspen simulation while additional costs such as labor and maintenance expenses are calculated based on chemical engineering heuristics [62]. The purchasing costs were estimated through the well-established

correlations and scaling factors reported in Seider [62], taking into consideration the required size and type of materials for each piece of equipment as well as the corresponding installation factor. All the costs were extrapolated to the 2022-dollar value using the Chemical Engineering Process Cost Index (CEPCI).

Based on these assumptions, the total capital investment (TCI) is calculated. TCI includes the

Current cost =
$$(\cos t \text{ in year i}) \frac{\text{Current Index}}{\text{Index in year i}}$$
 (1)

direct (equipment, installation, piping, etc.) and indirect costs (engineering, contractor fees, etc.) associated with the construction of a manufacturing facility. TCI also incorporates the working capital, which is the amount that should be available to finance the early operation of the plant.

Additionally, to complete the techno-economic analysis for the plant, estimations for the annual operating costs and sales profit are required. The cost of production is calculated as the sum of the cost of manufacture and general expenses which typically includes direct manufacturing costs (such as feedstocks, utilities, etc.), operating overhead, fixed costs (property taxes, depreciation, etc.), and general expenses (related with the central operation of the company). Prices of raw materials, products, and by-products are obtained from a recent study by Singh et al. [49] that provides a comprehensive analysis of the price trends over the previous decade. The average of prices reported between 2012-2016 are utilized in the context of this analysis. A detailed breakdown of all the prices used can be found in the SI (Table S9 and Table S10). The cost of pretreatment including shredding and cleaning of the postconsumer plastic bales is integrated in the price of PET flakes (\$0.55/kg). The complete set of prices is summarized in Table 3.

Table 3: Raw material, product, and utility prices.

	Cost (\$/kg)	Reference
Products		
TPA	1.14	[49]
Ethylene Glycol	0.96	[49]
Na ₂ SO ₄	0.15	[49]
Raw Materials		
PET	0.55	[49]
Acetone	0.91	[67]
NaOH	0.61	[49]
H ₂ SO ₄	0.10	[49]
Utilities		
Process water	\$ 0.27 /m ³	[62]
Cooling water	\$ 5 /GJ	[62]
Electricity	\$ 0.07/kW-h	[62]
Refrigerant	\$ 6.47/GJ	[62]

The Net Present Value (NPV) is an indicator often used to assess the profit potential of industrial processes[53,68]. The NPV represents the surplus generated by an investment at the beginning of the planning horizon relative to the return rate applied and provides insights into the time value of

money by discounting future cash flow to their present worth. To evaluate NPV, a discounted cash 245 flow analysis was conducted (Equation (2)).

$$NPV = -Z_0 + \sum_{t=0}^{T} \frac{Annual CF_t}{(1+RR)^t}$$
 (2)

244

249

250

251

252

253

254

255

256

257

258

259

Here, Z₀ represents the initial investment in \$, RR the rate of return, while CF_t denotes the annual 247 248 cashflow at time t.

In addition, we utilized the minimum selling price (MSP) as an economic indicator to facilitate comparisons between the proposed technology, competing processes, and present market prices. The MSP corresponds to the price that generates an NPV value equal to zero [68,69]. In other words, a break-even assessment was performed to identify the selling price of the main product (TPA) after which the process becomes profitable.

The depreciation method employed for this project is a 10-year MACRS, with a two-year startup time, with no profit during the first two years. The facility is assumed to operate at three 8 h/day shifts for 330 days/year. A return rate of 10% is utilized to evaluate the present value of future cash flows, while the inflation rate was set at 2%. All the financial parameters employed in this work are depicted in **Table 4**.

Table 4: Economic assumptions.

Parameter	Value
Feedstock rate	2000 kg/h
Annual interest rate	10 %

MACRS depreciation	10 years
Taxation rate	26%
Inflation rate	2%
Cost of land	3% of Purchase cost
Project life	12 years
Construction period	2 years
Working capital	5% of TCI
Maintenance	10% of TCI

3. Results and Discussion

3.1. Overview of the process flow diagram

Fig. 3 illustrates the simplified process flow diagram for the mechanochemical hydrolysis of PET waste, including the depolymerization reactor unit and all the subsequent product recovery steps. The designed facility processes 2000 kg/h (15,840 MT/year) of PET and generates approximately 1935 kg/h (15,325 MT/year) of terephthalic acid (TPA) and 737 kg/h (5840 MT/year) of ethylene glycol (EG), which can be utilized directly in the production of new PET products.

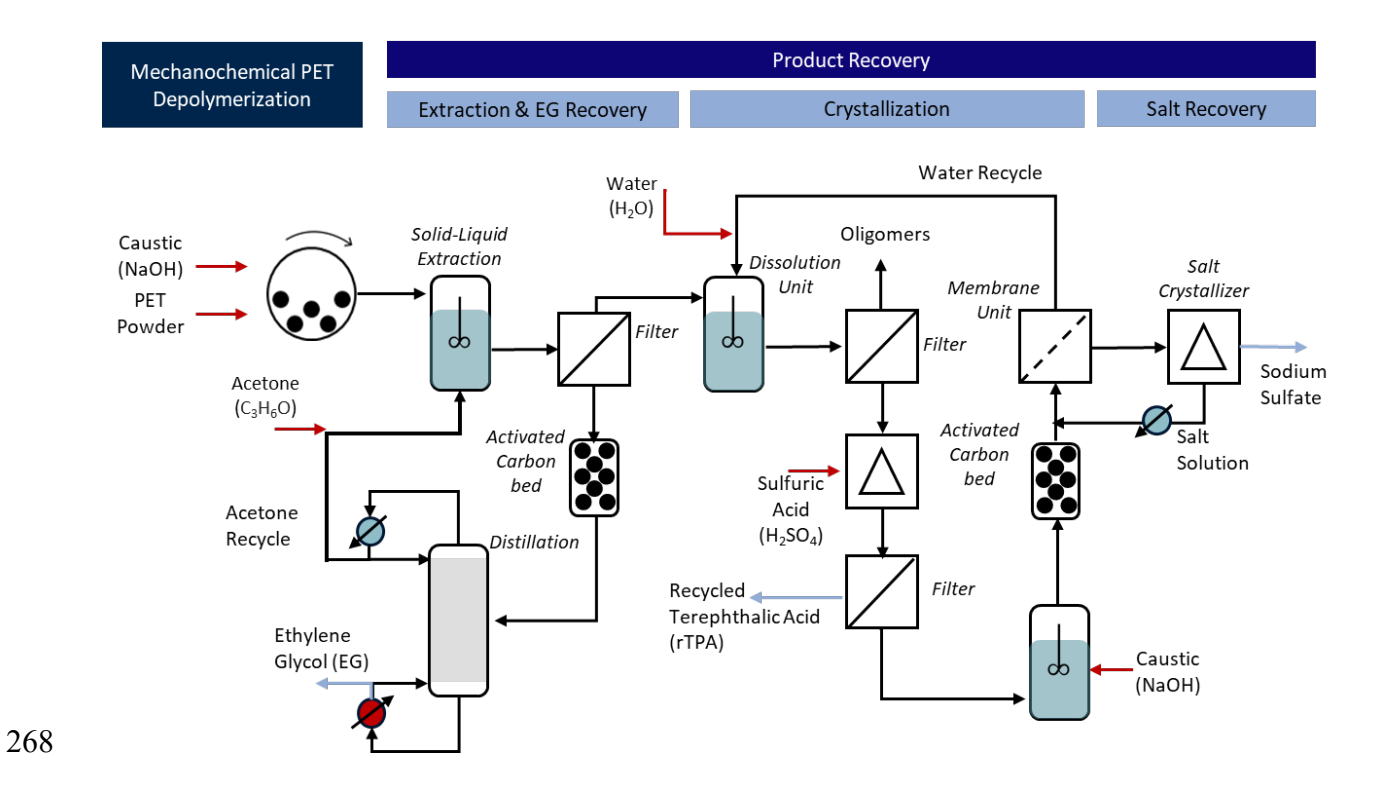


Fig. 3: Baseline case process for mechanochemical depolymerization of PET waste, divided into depolymerization and product recovery sections. Input streams are illustrated in red while product streams are in blue.

Clean PET powder flakes are obtained from a pre-treatment facility under the assumption that the whole feed is recyclable, and the concentration of impurities is negligible. As reported by Tricker et al. [19], high depolymerization yields ranging from 80 to 100 % were achieved in the ball mill reactor at the laboratory scale when using PET waste feedstock in the form of powder with particle sizes in the range of 0.3 mm for the operating setting that promote complete conversion as discussed in *Section 2.5*. The baseline analysis assumes the use of clean and uncontaminated PET flakes, providing a conservative estimate for the recycled terephthalic acid (rTPA) price. Depolymerization experiments were also conducted using commercial PET bottles and food

containers as inputs to illustrate the robustness of the process. Further discussion on the use of non-ideal feedstocks is provided in Sections 3.2 and 3.4. Prior to the depolymerization section, several feedstock pretreatment steps were also introduced to account for the cost required to transfer the PET flakes from storage to the reactor (conveyor belt, storage space and tanks, truck dumper). The pre-treatment steps were only accounted for in economics and were not simulated in Aspen Plus. The plastic waste powder is introduced into the ball mill reactor along with the NaOH particles and is converted into the monomers disodium terephthalate (Na₂TPA) and ethylene glycol (EG). Following the mechanochemical depolymerization reaction, the ball mill reactor outlet stream (e.g., Na₂TPA + EG) is processed through a solid-liquid extraction and a filtration unit. Acetone is used to selectively extract EG from Na₂TPA, and the resulting slurry is passed through a filter to separate the solids (Na₂TPA, additives, and any unreacted PET). An activated carbon column is installed to remove any dyes, pigments, or adhesives present in the acetone + EG stream. EG and acetone are then separated in a distillation column with a purity over 99% and 99%+ recovery. The Na₂TPA from the solids (Na₂TPA and unreacted PET), is selectively dissolved in water (H₂O) at a mass ratio of 1:9 and filtered to separate any residual PET. In the scenario that full depolymerization is not achieved, residual PET can be recycled back to the ball mill. Sulfuric acid (H₂SO₄) is then added slowly to the resulting aqueous solution of Na₂TPA to precipitate rTPA (recycled terephthalic acid) in a continuous crystallizer. The resulting rTPA crystals are then retrieved at a purity of 99%. The precipitation and filtration step recovers 97%+ of the monomer,

280

281

282

283

284

285

286

287

288

289

290

291

292

293

294

295

296

297

298

as observed experimentally. An activated column is installed to separate any traces of rTPA that were not collected from the aqueous solution.

The aqueous solution exiting the activated carbon column, is neutralized with caustic (NaOH) and processed in a reverse osmosis membrane unit with 63.6% water recovered. The permeate (process water) is returned to the dissolution unit, while the retentate is routed to a cooling crystallization unit for the recovery of sodium sulfate (SS). The SS crystals (also known as Glauber's salt) are produced and are collected as a byproduct. The saturated solution is recycled to the membrane to recover water and concentrate the SS aqueous solution (rerouted back to the salt recovery section).

Table 5 presents the feedstock, resulting product, and co-products mass flow rates, while Table 6 summarizes the reactions involved throughout the integrated process. A figure depicting the Aspen Plus simulation is provided in the SI (Fig. S5).

Table 5: Feed, product, and by-products quantities

	Unit	Baseline case
PET waste feed	kg/h	2000
rTPA product	kg/h	1935
By-products		
Ethylene glycol	kg/h	737
Sodium sulfate	kg/h	3866

Table 6: Reactions involved in the process.

Unit	Stoichiometry
Ball mill	$rPET + 2NaOH \rightarrow C_2H_6O_2(EG) + Na_2TPA$
Acidification	$Na_2TPA + H_2SO_4 \rightarrow TPA + Na_2SO_4$
Neutralization	$H_2SO_4 + 2NaOH \rightarrow Na_2SO_4 + 2H_2O$
Crystallization	$Na_2SO4 + 10 H_2O \rightarrow Na_2SO4 \cdot 10 H_2O$

3.2. Experimental Results

Fig. 4 shows the solution NMR data of the depolymerized mixture, filtrate after EG extraction with acetone, and filtered solids in D₂O. Equimolar concentrations of terephthalate (~7.8 ppm) in the form of Na₂TPA and EG (~3.5 ppm) were observed in the spectrum of depolymerized PET. The absence of the aromatic proton peak corresponding to Na₂TPA or any unreacted PET in the spectrum of the filtrate indicates the excellent selectivity of EG extraction with acetone. The solution NMR data analysis with DSS as the internal standard showed 98% EG recovery. A 1:1 ratio by weight of EG to acetone was used for extraction at the laboratory scale. Since EG is miscible in acetone, this ratio was used to provide effective mixing of reactor product solids with acetone (**Fig. S1**, Supporting Information). EG was recovered with 99 mol% purity with a rotary evaporator (370 mbar, 50 °C) mimicking a single-stage distillation.

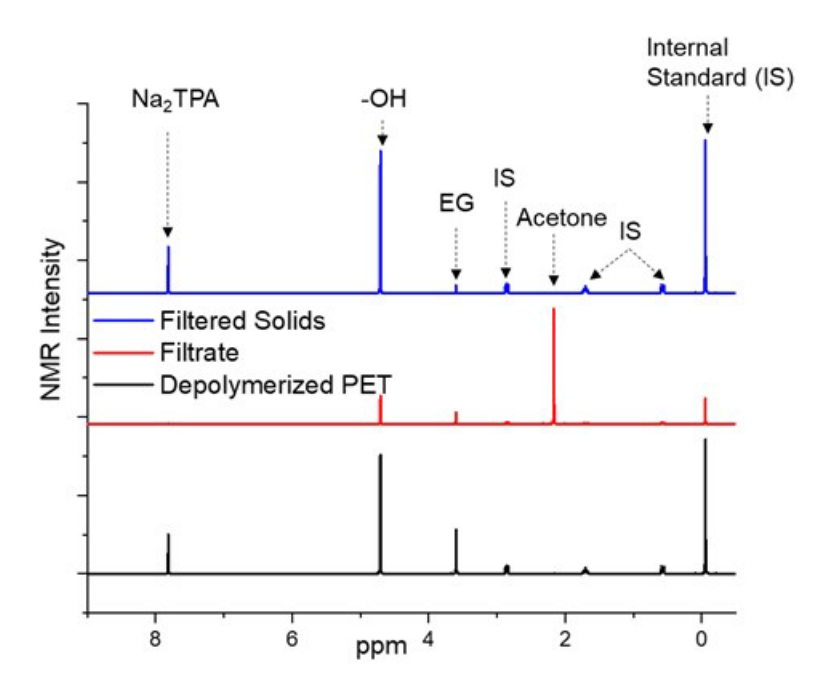


Fig. 4: Solution NMR spectra (in D₂O) of depolymerized PET (black), EG-acetone extraction filtrate (red), and filtered solids (blue).

To further test the robustness of the process, waste PET textile (with brown dye) from Kolon Industries were tested. Although the presence of dyes in commercial textile samples does not affect the efficiency of extraction of EG with acetone, a significant amount of dye disperses in the acetone phase (Fig. S2a). Activated carbon adsorbents selectively remove the dispersed dyes from the acetone phase (Fig. S2a). These observations are supported by the solution NMR spectrum (Fig. S2b) which shows the presence of characteristic dye peaks (~2.13 ppm) in the acetone phase, and the subsequent disappearance of such peaks after treatment with activated carbon. Complete dissolution of the filtered solids (predominantly Na₂TPA with complete depolymerization) was observed by maintaining the concentration under 10 wt% at room temperature. Residual dye (in commercial samples) dispersed in aqueous Na₂TPA solution was selectively removed with

activated carbon (Fig. S3). Additionally, the depolymerization of commercial PET bottles and food containers was also studied (Fig. S4a). Near complete depolymerization of both PET bottles and food containers were obtained withing 20 mins of ball milling (Fig. S4b). Furthermore, solution NMR spectrums of both PET bottles and containers (in TFA-d) show no additives or contaminants (Fig. S4c). Fig. S4d shows the absence of any byproducts (except EG and Na₂TPA) after complete depolymerization of PET bottles and containers. Thus, the proposed process flow and techno-economic analysis are robust towards commercial feed stock such as waste PET textile, PET bottles and food containers. The precipitation of TPA was performed with the slow acidification of aqueous Na₂TPA solution with slight excess of H₂SO₄ (1.003 times stoichiometric). Solution NMR confirmed 98% recovery of terephthalic acid from the completely depolymerized PET, similar to earlier observations.[70] Fig. 5a shows the powder XRD pattern of the recovered crystals. The presence of characteristic crystalline peaks confirms the formation of TPA crystals. Fig. 5b compares the NMR spectra of pure and recovered TPA in DMSO-d₆. No significant peaks other than TPA, H₂O, and DMSO can be identified, confirming the excellent purity of rTPA. Fig. 5c and 5d show magnified plots from Fig. 5b, in which the small peaks present are due to noise/instrumental artifacts.

338

339

340

341

342

343

344

345

346

347

348

349

350

351

352

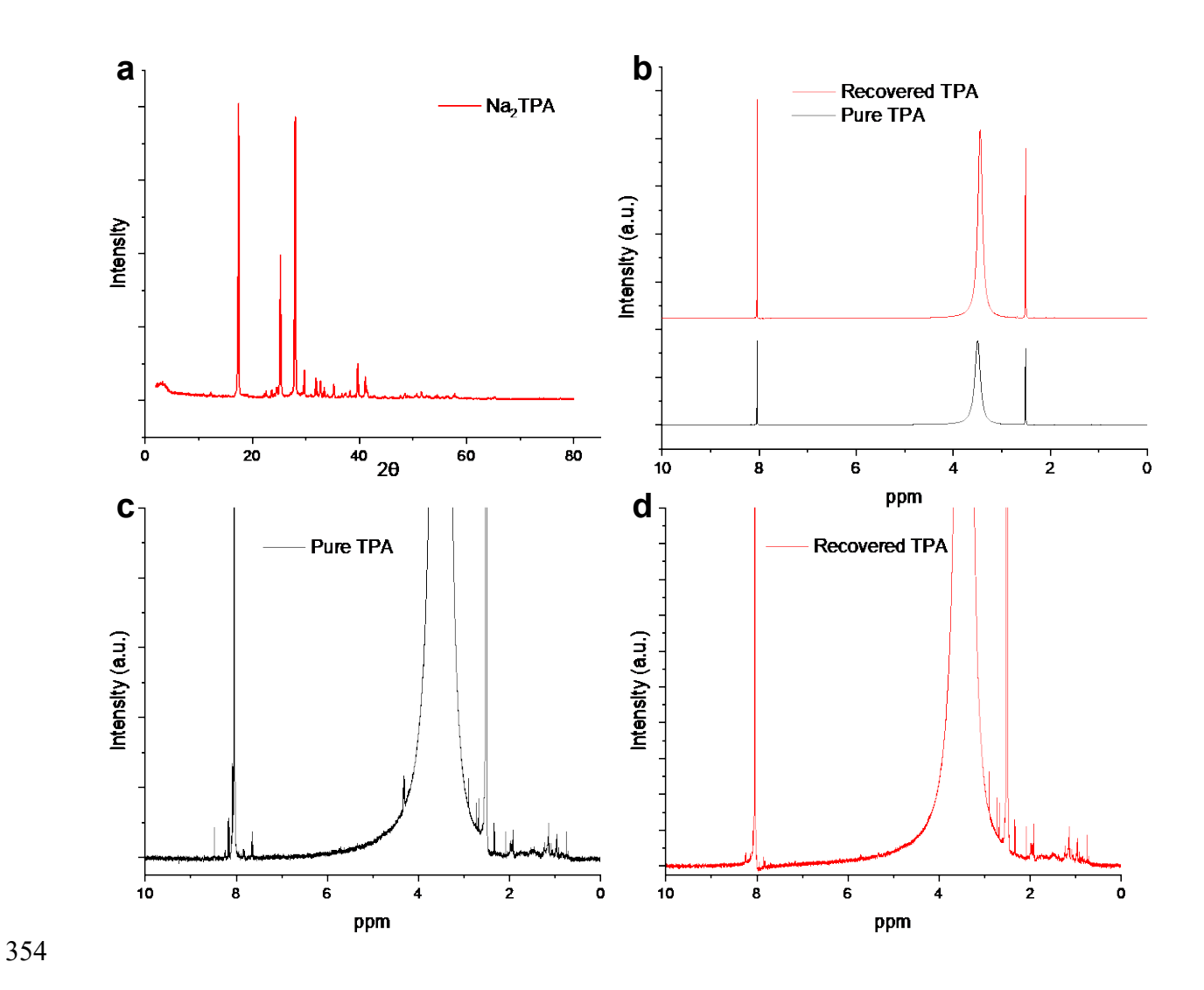


Fig. 5: (a) Powder XRD pattern of recovered TPA, (b) NMR spectra of pure and recovered TPA in DMSO-d₆, (c) and (d) magnified NMR spectra of pure and recovered TPA respectively.

The recovery of process water was demonstrated with a DuPont XC70 reverse osmosis membrane. The supernatant was neutralized with the addition of stoichiometric NaOH to enhance salt rejection performance. Table 7 shows the salt rejection performance and the flux of process water at 70 bar and room temperature. A feed concentration of 72.73 g/L depicts the initial feed concentration

after rTPA precipitation. The 200 g/L of Na₂SO₄ solution represents the brine (end of membrane stage) with ~63.6% water recovered. Significant salt rejections were observed (~95.7%) at both the starting and brine concentrations. Li et al. also showed similar results with a commercial RO membrane.[71] These data were used to model a membrane unit for water recovery.

Table 7: Na₂SO₄ salt rejection performance of DuPont XC70 membrane

Feed Concentration (g/L)	Water Flux (L/m²/hr)	Salt Rejection (%)
72.73	31.0	96
250	3	92

3.3. Process simulation and Economic analysis

Equipment sizes, and subsequently the overall capital investment, were evaluated based on the mass and energy flows obtained from the process simulation. Information on raw materials flows and energy requirements was utilized to calculate the variable operating costs. The resulting mass flows are summarized in **Table S1 – S5** and **Fig. S5**. The TCI is projected at \$10.6M, while the bare module cost (**Fig. 6**) is estimated at \$6.2M. The highest contribution (62%) to the bare module cost is attributed to the product purification steps such as EG distillation, recovery of the rTPA crystals, and Glauber's salt crystallization, and this is mainly due to the capital cost of the distillation column and the salt crystallizer. The initial capital expenses for the downstream separation units are mitigated by the EG and SS stream recovery, which are subsequently sold at their market price. In addition, 21% of the TCI is estimated for the pretreatment steps that include the necessary machinery for feedstock transportation and storage. The depolymerization section, which includes the ball-mill reactor, accounts for 17% of the total capital expenditure. **Table 8**

provides a detailed cost breakdown for each unit operation modeled as well as the capital costs (bare module) for each section.

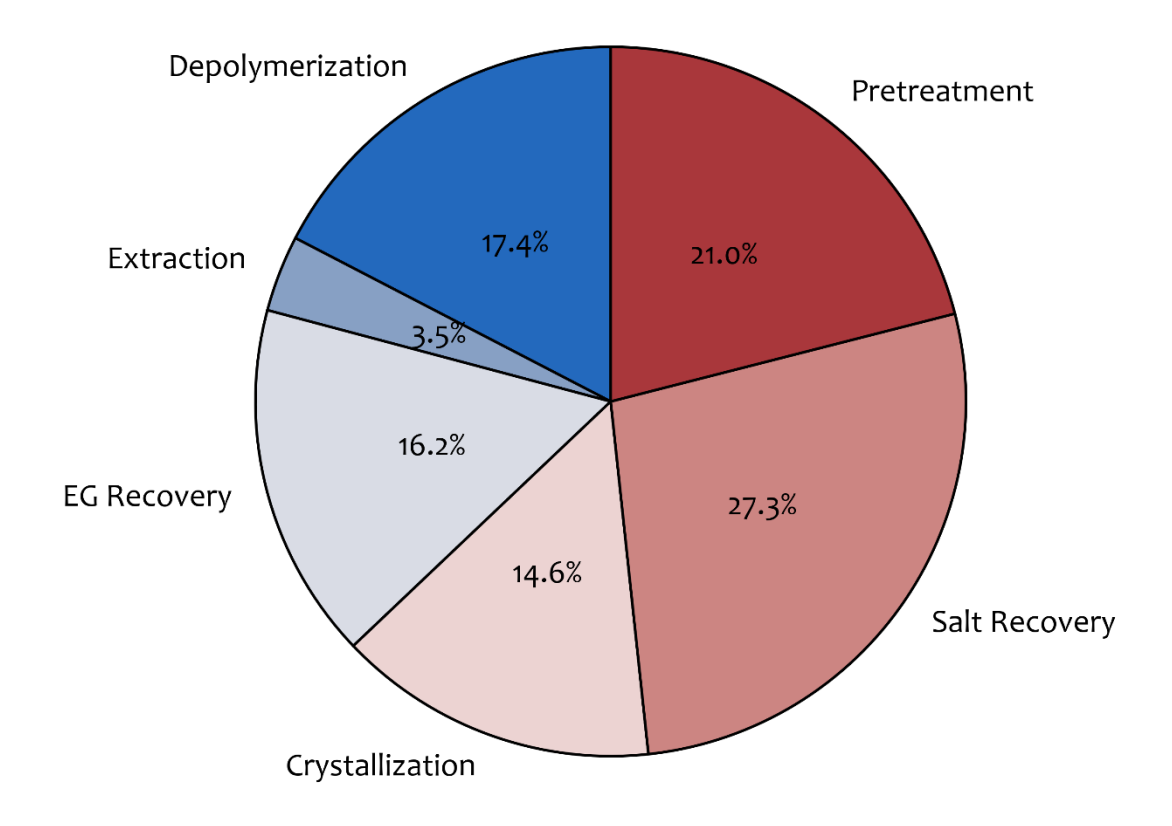


Fig. 6: The bare module cost of \$6.2M split into different process sections.

Table 8: Capital cost (bare module) breakdown for all the processing units.

Capital cost (\$)		Capital cost (\$)	
Pretreatment	\$1,309,771	Crystallization	\$909,581
Conveyor belt	\$31,486	Dissolution	\$156,121

NaOH tank	\$98,243	Filter 2	\$127,017
Truck dumper	\$283,508	Filter 3	\$125,184
Storage dome	\$896,534	Acidification	\$191,650
Depolymerization	\$1,082,976	TPA tank	\$181,984
Ball Mill	\$1,082,976	H2SO ₄ tank	\$127,625
Extraction	\$216,695	Salt Recovery	\$1,700,779
Extraction Unit	\$129,754	Membrane	\$352,479
Filter 1	\$47,742	Crystallization	\$457,762
AC1	\$5,288	Neutralization reactor	\$220,184
Acetone tank	\$33,912	Pump 2	\$300,403
EG recovery	\$1,012,525	SS Filter	\$81,632
Distillation column	\$872,861	AC2	\$25,278
EG tank	\$139,664	SS tank	\$263,041

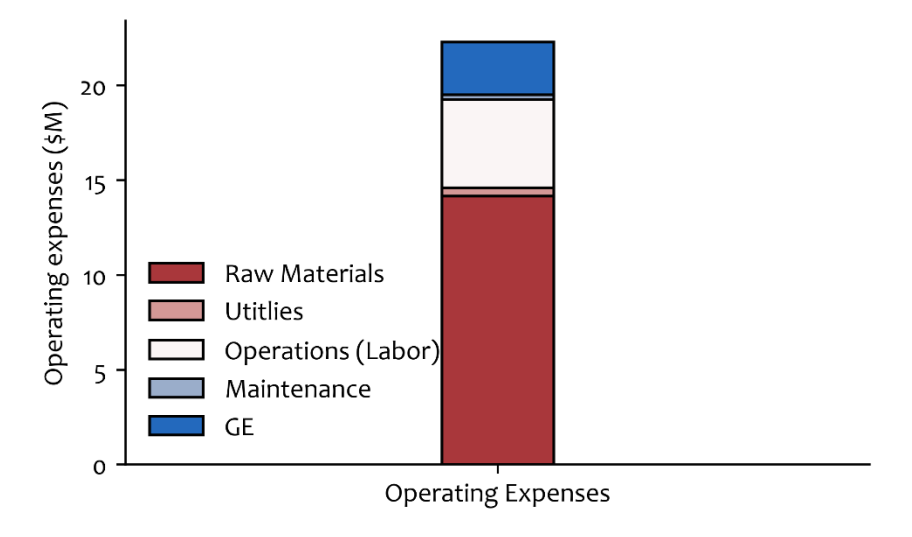


Fig. 7: Operating expenses breakdown.

Other than the upfront equipment investment, an annual operating cost of \$22 M USD is required for the efficient operation of the facility. As illustrated in Fig. 7, the primary component of the operating expenses is the cost of raw materials. Particularly, the cost of feedstock accounts for 62% of the raw material costs. In the baseline analysis, it is assumed that the feedstock is derived from the use of clean PET flakes sourced from PET recyclers. The implementation of a pretreatment section at the production facility, that would shred and clean the PET bales (compressed plastic waste), could significantly reduce the cost of raw materials. More specifically, PET bales are priced at approximately one-sixth the cost of clean flakes, hence, there is potential to make the process even more profitable. As illustrated experimentally, the proposed design is capable of processing commercial waste, demonstrating the practical feasibility of reducing the feedstock cost. Another notable advantage of mechanochemical depolymerization is that it does not require fine particles as feedstock since the sizes of the plastics are further reduced during the ball milling process.

The consumption of electricity is a major cost factor in the depolymerization section, primarily required to power the rotation of the milling vessel and the grinding balls. In the crystallization section, the primary cost drivers are the chemicals used for the recovery of rTPA crystals, which are offset by the recovery of sulfuric salt in the subsequent process section. Similarly, in the distillation column, the high quantity of steam required for the evaporation of acetone is balanced with the recovery of EG. Additionally, replacement costs for the grinding balls of the ball mill reactor, membrane replacement (every 4 years in the baseline case), activated carbon bed are also accounted for in the economic analysis and are counted as operating expenses. The broad categories of costs and revenue are shown in **Table 9**.

Table 9: Main costs and sales revenues for baseline mechanochemical plant (2000 kg/h PET).

Category	Amount
Total capital investment (TCI)	\$10,587,425
Cost of Manufacturing (COM)	\$20,514,329
Total utility costs	\$446,111
Total raw materials	\$14,159,020
Total product sales	\$27,668,595

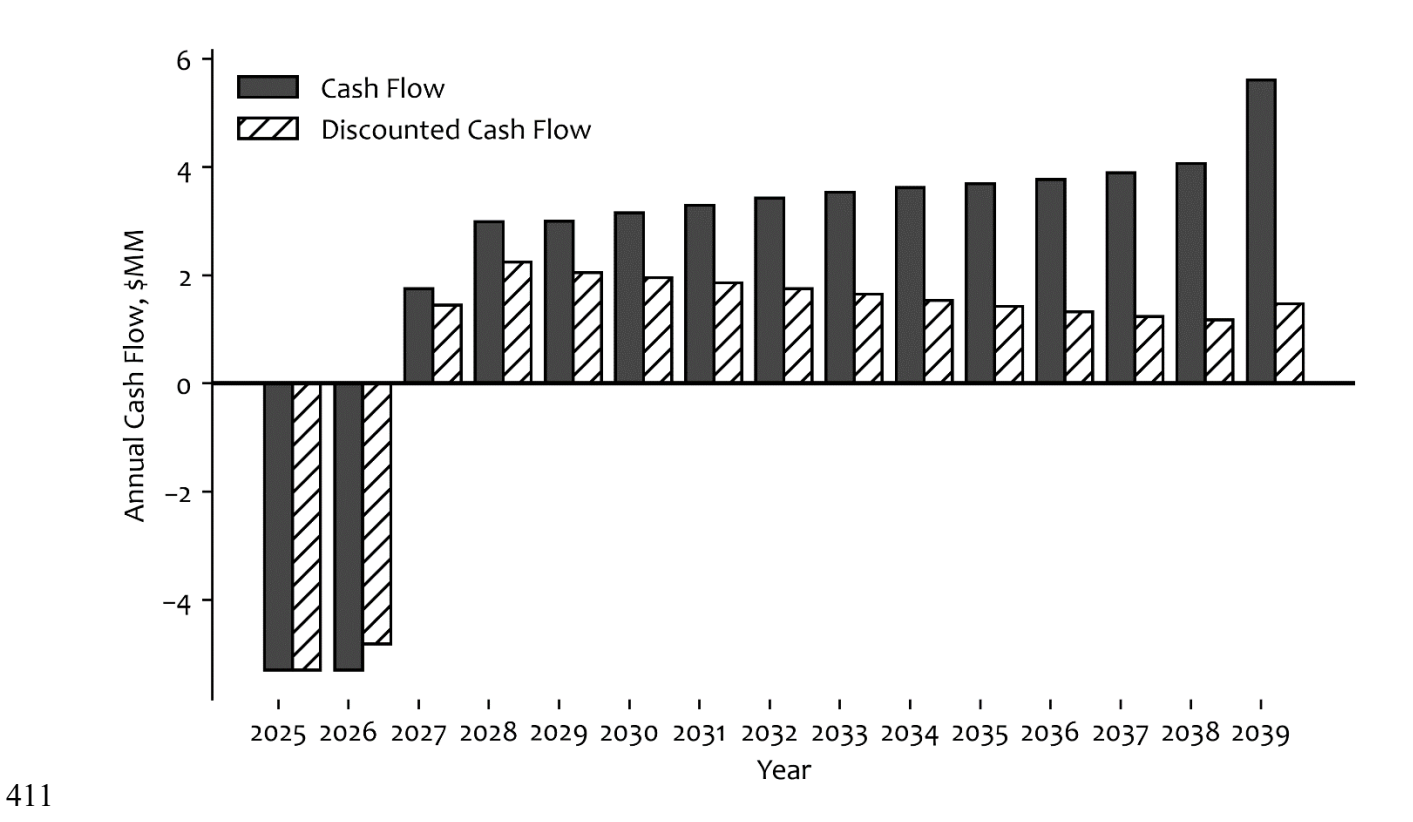


Fig. 8: Annual cash flow in \$M for 12 years of operation. The first two years are for commissioning, and hence the sales are zero.

A discounted cash flow analysis approach was implemented to evaluate the projected break-even point and the rTPA minimum selling price (MSP) produced in this facility, accounting for the revenue from ethylene glycol (EG) and Glauber salt (SS) sales. The net-present-value (NPV) and minimum selling price (MSP) profitability metrics are determined based on the assumptions discussed in a previous section. An MSP of \$0.99/kg for rTPA is estimated for the baseline case, indicating that the mechanochemical depolymerization process is competitive with the traditional vTPA (market price is \$1.14/kg). In essence, without accounting any profits and considering the

assumed market conditions, rTPA is found to be less expensive than fossil derived TPA. **Fig. 8** illustrates the cash flow and discounted cash flow of the baseline process, revealing that the process is profitable even for the scenario that ideal feedstock is used.

3.4. Sensitivity Analysis

To obtain further insights to the feasibility of the process, a single-point sensitivity analysis is conducted focusing on key-process and economic variables within each section. Through this approach, the potential for additional R&D can be identified and the most significant challenges for commercial success can be emphasized. The engineering parameters and economic assumptions were varied to assess profitability under different scenarios and uncertainty conditions in a plant-scale operation.

Table 10 summarizes the key parameters and their respective upper and lower bounds, that are expected to significantly impact the projected profitability and are therefore selected for sensitivity analysis. In terms of the reactor consumables, the grinding media lifetime is investigated by varying the degree of wear and tear of the stainless-steel balls. In the case of the reverse osmosis (RO) membrane, its lifespan is selected as a key design parameter. The crystallization temperature is also investigated since it determines the use of an expensive refrigerant (available at -12.2 °C) or cheaper cooling water (available at 4.4 °C) alternative as a cooling medium [58]. Finally, prices of PET bales (feed), raw materials (NaOH), and co-products (EG, SS) are also evaluated to assess their effect on the calculated economic metrics as all these prices are subject to volatility [49]. Their lower and upper bounds were set at +/- 20% of the baseline price, except for the price of

PET waste. A lower bound of \$ 0.2 /kg and \$ 1.0 /kg was set for the feedstock to investigate the scenarios that non-ideal feedstocks are used (e.g., PET bales).

In this analysis, we have varied each of the input sensitivity parameters (Table 10) one at a time, which does not account for the impact of parameter correlations on the robustness of the process economics. To justify this approach, a correlation analysis was conducted on historical price data and revealed no significant correlations. A table of historical prices used is provided in the SI (Table S9 – Table S10). With regards to the process-related sensitivity parameters (i.e., grinding media loss, membrane lifetime, crystallization temperature), no correlation is assumed since these can be independently varied within different unit operations. Therefore, in this study, all the parameters considered are assumed to be independent.

Table 10: Process sensitivity parameters.

Process-specific sensitivity parameters	Base case	Lower bound	Upper bound
Grinding media loss (g/MT media)	50	10	100
RO membrane lifetime (years)	4	1	6
SS Crystallization temperature (°C)	14.4	0.0	14.4
Waste PET price (\$/kg)	0.55	0.20	1.00
Co-product price – EG (\$/kg)	0.96	-20%	+20%
Co-product price – SS (\$/kg)	0.15	-20%	+20%
Raw material price – NaOH (\$/kg)	0.61	-20%	+20%
Raw material price – H ₂ SO ₄ (\$/kg)	0.10	-20%	+20%

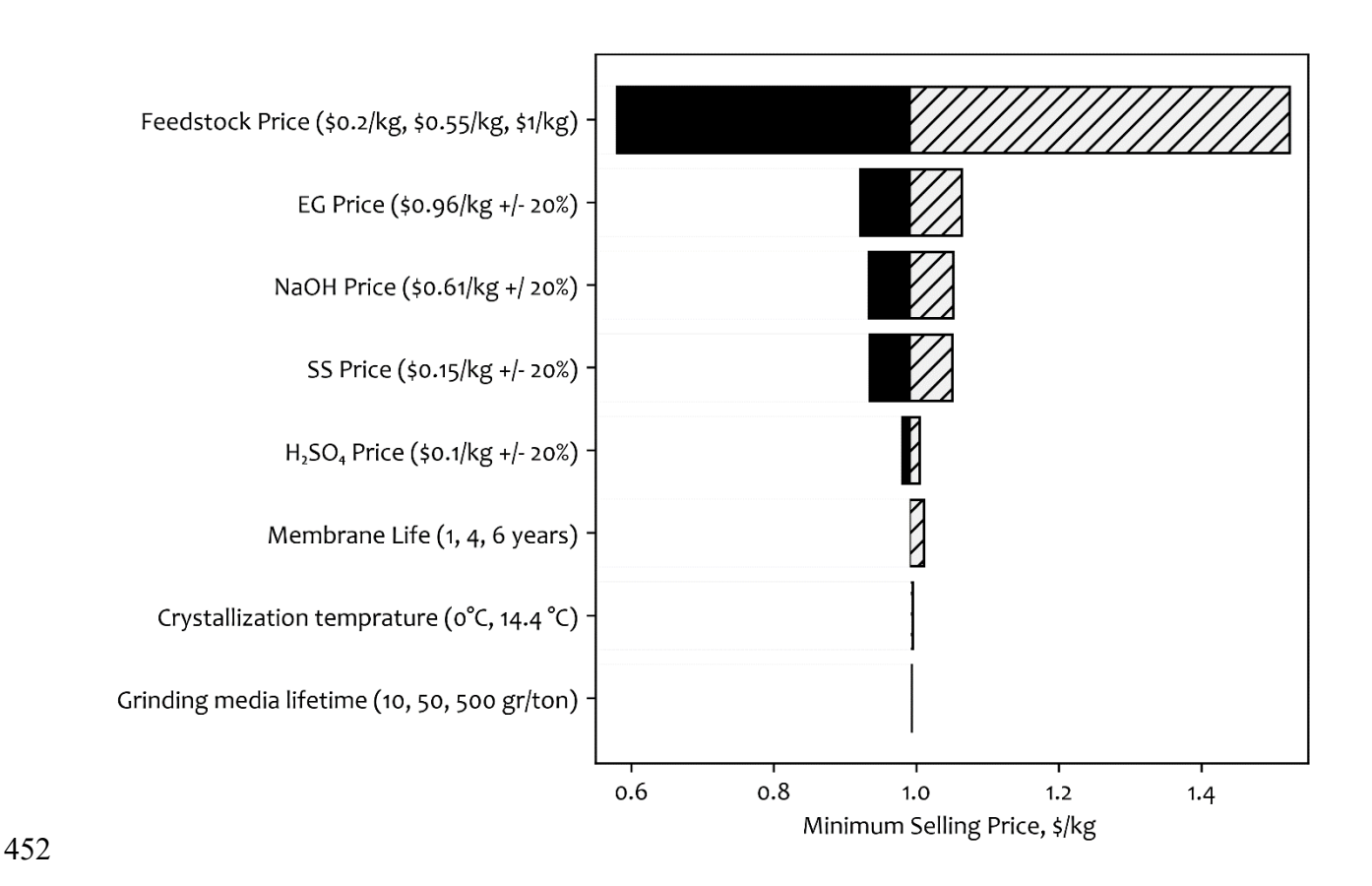


Fig. 9: Change in the TPA MSP as a function of prices of products, co-products, and raw materials; and key process parameters.

Fig. 9 depicts the impact of the prices of feedstock (PET), co-products (EG,SS), and raw materials (NaOH, H₂SO₄) on the MSP of rTPA. The MSP of the rTPA product is observed to exhibit high sensitivity to the price fluctuations of the waste PET. The NaOH price also has a strong effect on the MSP since it is utilized in large quantities in the depolymerization and salt recovery section. The selling prices of co-products such as EG or SS also appear to impact the price of the final product since they are both sold in high quantities. Finally, the price of H₂SO₄ appears to have minor effect to the resulting MSP, since it is relatively inexpensive compared to all others.

In terms of the process parameters (crystallization temperature, lifespan of the membrane, and the grinding media loss), they all exhibit a minor effect on the MSP compared to the other parameters. This result is attributed to the substantial impact of raw material prices on the overall operating expenses. In fact, the cost of raw materials constitutes 64 % of the total operating cost while the utilities only 2 % of the total operating cost.

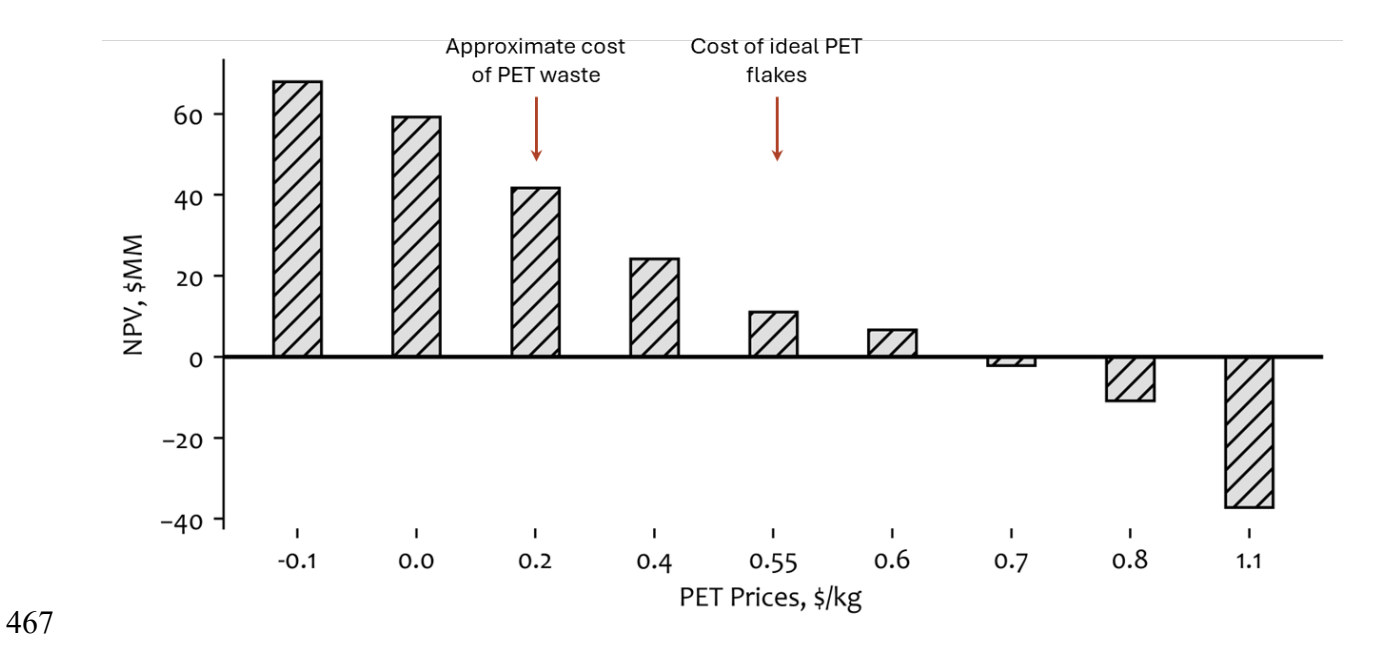


Fig. 10: Net Present Value (NPV) of the mechanochemical process for different waste PET prices.

Given the relatively high PET waste price volatility over the past decade [49], we performed a detailed sensitivity study covering a range of prices from -\$0.1/kg to \$1.1/kg to delve deeper into its effect to the process profitability. Negative prices indicate the scenario that incentives are provided to avoid landfilling and promote recycling. As illustrated in **Fig. 10**, the price of PET feedstock exhibits a linear relationship with the process NPV, with an identified break-even point at a price of \$0.68/kg for the PET feedstock given the assumed market prices. Beyond this

feedstock price, the NPV becomes negative indicating an unprofitable process. Conversely, below the price of \$0.68/kg the processes becomes profitable.

Notably, the modeled feedstock consists of clean PET flakes with very small particle sizes and are impurities-, dye- and dirt-free are ideal. Based on experimental results, the ball mill reactor can effectively process PET waste of various shapes, sizes, or sources without any impact to the observed conversion or additional pre-milling required since all reactants are milled as processed in the reactor. Therefore, the use of prices of PET bales as feedstock is expected to be representative of an actual industrial application, and the NPV values obtained in **Fig. 10** are applicable to such a scenario.

3.5. Technology comparisons

From an economic perspective and under the market assumptions considered in this assessment, the introduction of the mechanochemical PET depolymerization process in the recycling grid is economically profitable. A rTPA MSP of \$0.99/kg was evaluated for mechanochemical milled PET, a price that is directly comparable with the current prices of virgin TPA monomers. In **Table 11**, we report the MSPs of our proposed design with competing technologies as investigated by Uekert et al. [58]. In both studies, similar assumptions were made with respect to the quality of the feed and final products, the prices of raw materials retrieved from the same source, and similar processing sections were modeled. For the case of methanolysis, we report the price of dimethyl-terephthalate (DMT) which is the monomer that is used in the production of rPET. It is important to note that these estimates are based on published studies, thus we are not able to estimate uncertainty ranges for these numbers. However, to the best of our knowledge, the resulting MSPs

of the fossil- and recycled-based monomers reported in **Table 11** are comparable with our study since they account for the same process system boundaries. Uekert et al. [58] also evaluated the MSPs for glycolysis (\$0.96/kg) and dissolution (\$0.87/kg), however, their analysis included a repolymerization step at the end of the process sequence to produce rPET, so a direct comparison with the other methods would be unfair. This comparison indicates that the mechanochemical process for PET recycling (as modeled in this study) is expected to be competitive with other closed-loop recycling methods. It is worth noting that both actual selling prices and estimated MSPs highly depend on the market dynamics, supply chain, legislation, and demand for recycled monomers.

Table 11: Estimated MSP for different PET recycling processes.

Technology	MSP (\$/kg)	Reference
Virgin	1.14	[49]
Mechanochemical hydrolysis	0.99	This study
Enzymatic hydrolysis	1.96	[49]
Methanolysis (DMT price)	0.96	[58]

The facility size is also expected to drive down the capital and operating costs and increase cost savings by leveraging the benefits of the economies of scale. This applies to all closed-loop recycling technologies that are compared here. As landfilling is increasingly being banned entirely across Europe[72,73], and some US states [74] there will be a growing interest in managing the waste that cannot be landfilled. The smooth operation of any chemical facility is dependent on the

steady flow of the feedstock and raw materials hence, the current trend of increased recycling rates is expected to boost the operation of the recycling facility and increase savings.

511

512

513

514

515

516

517

518

519

520

521

522

523

524

525

526

527

528

529

530

531

Mechanochemical recycling is shown here to be a promising technology that could claim a significant share of the current recycling market. This method offers the advantage of high conversion without the need for extreme conditions or pretreatment steps to pre-mill plastic waste to the micron scale. Other plastic feedstocks and depolymerization kinetics should be investigated to enable the holistic investigation of the economic impact of this method in comparison with other recycling technologies. While the operating conditions of the ball mill reactor influence the effectiveness of PET waste depolymerization (e.g., partial or complete depolymerization), efficient separation of products/co-products significantly influences the MSP. In the proposed design any dyes, pigments or adhesives that may be present in the feed are passed through the activated carbon columns and are efficiently removed. Hence, minimizing consumables such as solvents, electricity, steam, and NaOH, many of which are used for the subsequent separation procedures for product recovery, will allow further cost savings. For example, the use of nanofiltration (NF) and RO membranes in series for water recovery could be advantageous, since the NF stage may retain a large fraction of the salt and produce usable water with high flux and lower operating pressure, leaving a much lower volume of NF retentate to be processed by RO to produce additional water. Furthermore, periodic regeneration of the activated carbon bed (before the Na₂SO₄ crystallizer) with recovered process water will additional rTPA. Additionally, the optimization of acetone required for the extraction of EG (at large industrial scale) will significantly reduce distillation costs.

4. Conclusions

532

533

534

535

536

537

538

539

540

541

542

543

544

545

546

547

548

549

550

551

552

In this work, we presented an integrated approach to demonstrate the technical and economic potential of mechanochemical depolymerization of PET. A sequence of unit operations for the downstream purification steps following the ball-mill reactor was designed, experimentally validated at the laboratory scale, and simulated in Aspen Plus. The process flow presented herein enables significant recovery of both TPA (~97%) and EG (~99%) as compared to other chemical recycling technologies. Ideal (PET powder) and commercial (bottles, food containers, textiles) samples were examined and used as feedstock to the process. The integrated process is shown to be resilient towards the presence of impurities (such as dyes and pigments) in the feedstock or the use of commercial plastic waste as feedstock (such as textiles, food-grade bottles, and containers). The product quality of rTPA obtained from the mechanochemical recycling process is comparable to petroleum-derived TPA, as opposed to the current industry-standard mechanical recycling. A techno-economic analysis was also conducted to assess the overall economic viability and critical factors that impact the economics of the process. The findings of the analysis revealed a positive NPV and an evaluated MSP of \$0.99/kg for the baseline scenario that utilizes clean PET powder as feedstock. Feedstock prices and purification steps account for a large portion of the operational and capital expenditures, respectively. The downstream purification steps dictate the final selling price of rTPA, as their integration with the reactor enables the efficient recovery and sale of co-products in large quantities. Results from sensitivity analysis show that the process is highly sensitive to the prices of feedstock and raw materials. In the investigated scenarios that PET waste bales are purchased and used as inputs instead of ideal clean PET powder, the process

becomes even more profitable. Furthermore, the process designed in this manuscript is competitive with conventional fossil-based sources and alternative recycling pathways as the calculated MSP is at par with the vTPA and rTPA prices. While the framework outlined in this work primarily targets PET waste, a similar mechanochemical or mechanocatalytic approach can be applied to other waste polymer feedstocks.

Finally, it should be noted that the models utilized in this study are based on conversions observed at the laboratory scale. To account for deviations and additional degrees of freedom of the process sequence at larger scale, future work will include the development of detailed models and further experimentation. Moreover, the combination of process, supply chain, and life cycle assessment (LCA) will enable a full evaluation of the environmental factors and social-economic impacts of this technology, such as GHG emissions. This will enable a holistic comparison of mechanochemical depolymerization relative to other recycling technologies and allow the identification of an optimal supply chain of recycling processes. The outcome of the analysis presented herein provides yield and economics metrics for a complete mechanochemical process for recycling of PET waste. Such studies are necessary to assess the potential feasibility of new technologies, and for developing policies that incentivize industries to pursue pathways that promote chemical recycling, in anticipation of the transition to a complete circular economic model for plastics.

Declaration of Competing Interest

The authors declare the following financial interests/personal relationships which may be considered as potential competing interests: Carsten Sievers, Sankar Nair, Christopher Jones, and

- 574 Fani Boukouvala have a provisional patent application filled in the U.S. Patent and Trademark
- Office as U.S. Patent Application serial No.: 17/801,027 to Georgia Tech Research Corporation.

Data Availability

576

578

Data will be made available on request.

Acknowledgement

- 579 The work was financially supported by Kolon Industries, Inc. through the Kolon Center for
- Lifestyle Innovation at Georgia Institute of Technology, and the U.S. National Science Foundation
- Emerging Frontiers in Research and Innovation program under grant 2028998.

582 Appendix A. Supporting Information

- The Supporting Information document contains additional experimental data and technoeconomic
- analysis results.

585 References

- 586 [1] R. Geyer, J.R. Jambeck, K.L. Law, Production, use, and fate of all plastics ever made, Sci
- 587 Adv. 3 (2017) 25–29. https://doi.org/10.1126/sciadv.1700782.
- [2] I. Vollmer, M.J.F. Jenks, M.C.P. Roelands, R.J. White, T. van Harmelen, P. de Wild, G.P.
- van der Laan, F. Meirer, J.T.F. Keurentjes, B.M. Weckhuysen, Beyond Mechanical
- Recycling: Giving New Life to Plastic Waste, Angew Chem Int Ed Engl. 59 (2020) 15402–
- 591 15423. https://doi.org/10.1002/anie.201915651.

- 592 [3] L.E. Revell, P. Kuma, E.C. Le Ru, W.R.C. Somerville, S. Gaw, Direct radiative effects of
- 593 airborne microplastics, Nature. 598 (2021) 462–467. https://doi.org/10.1038/s41586-021-
- 594 03864-x.
- 595 [4] L.C. Jenner, J.M. Rotchell, R.T. Bennett, M. Cowen, V. Tentzeris, L.R. Sadofsky, Detection
- of microplastics in human lung tissue using µFTIR spectroscopy, Science of the Total
- 597 Environment. 831 (2022). https://doi.org/10.1016/j.scitotenv.2022.154907.
- 598 [5] P.S. Ross, S. Chastain, E. Vassilenko, A. Etemadifar, S. Zimmermann, S.A. Quesnel, J.
- 599 Eert, E. Solomon, S. Patankar, A.M. Posacka, B. Williams, Pervasive distribution of
- polyester fibres in the Arctic Ocean is driven by Atlantic inputs, Nat Commun. 12 (2021).
- 601 https://doi.org/10.1038/s41467-020-20347-1.
- 602 [6] T. Tiso, T. Narancic, R. Wei, E. Pollet, N. Beagan, K. Schröder, A. Honak, M. Jiang, S.T.
- Kenny, N. Wierckx, R. Perrin, L. Avérous, W. Zimmermann, K. O'Connor, L.M. Blank,
- Towards bio-upcycling of polyethylene terephthalate, Metab Eng. 66 (2021) 167–178.
- 605 https://doi.org/10.1016/J.YMBEN.2021.03.011.
- 606 [7] H. Li, H.A. Aguirre-Villegas, R.D. Allen, X. Bai, C.H. Benson, G.T. Beckham, S.L.
- Bradshaw, J.L. Brown, R.C. Brown, V.S. Cecon, J.B. Curley, G.W. Curtzwiler, S. Dong, S.
- Gaddameedi, J.E. García, I. Hermans, M.S. Kim, J. Ma, L.O. Mark, M. Mavrikakis, O.O.
- Olafasakin, T.A. Osswald, K.G. Papanikolaou, H. Radhakrishnan, M.A. Sanchez Castillo,
- K.L. Sánchez-Rivera, K.N. Tumu, R.C. Van Lehn, K.L. Vorst, M.M. Wright, J. Wu, V.M.
- Zavala, P. Zhou, G.W. Huber, Expanding plastics recycling technologies: chemical aspects,

- 612 technology status and challenges, Green Chemistry. 24 (2022).
- 613 https://doi.org/10.1039/d2gc02588d.
- 614 [8] Z. Jagiello, M. Corsini, Ł. Dylewski, J.D. Ibáñez-Álamo, M. Szulkin, The Extended Avian
- Urban Phenotype Impact of Anthropogenic Debris Pollution on Nest Design and Fitness,
- SSRN Electronic Journal. (2022). https://doi.org/10.2139/SSRN.4020176.
- 617 [9] K.R. Nicastro, L. Seuront, C.D. McQuaid, G.I. Zardi, Symbiont-induced intraspecific
- phenotypic variation enhances plastic trapping and ingestion in biogenic habitats, Science
- of The Total Environment. 826 (2022) 153922.
- 620 https://doi.org/10.1016/J.SCITOTENV.2022.153922.
- 621 [10] J.M. Sipe, N. Bossa, W. Berger, N. von Windheim, K. Gall, M.R. Wiesner, From bottle to
- microplastics: Can we estimate how our plastic products are breaking down?, Science of
- 623 The Total Environment. 814 (2022) 152460.
- 624 https://doi.org/10.1016/J.SCITOTENV.2021.152460.
- 625 [11] A.N. Walsh, C.M. Reddy, S.F. Niles, A.M. McKenna, C.M. Hansel, C.P. Ward, Plastic
- Formulation is an Emerging Control of Its Photochemical Fate in the Ocean, Environ Sci
- 627 Technol. 55 (2021) 12383–12392.
- 628 https://doi.org/10.1021/ACS.EST.1C02272/SUPPL FILE/ES1C02272 SI 001.PDF.
- 629 [12] Researchers Engineer Microorganisms To Tackle PET Plastic Pollution | News | NREL,
- 630 (n.d.). https://www.nrel.gov/news/program/2021/researchers-engineer-microorganisms-to-
- tackle-pet-plastic-pollution.html (accessed March 10, 2022).

- 632 [13] J.M. Garcia, M.L. Robertson, The future of plastics recycling, Science (1979). 358 (2017)
- 633 870–872.
- 634 [14] T. Thiounn, R.C. Smith, Advances and approaches for chemical recycling of plastic waste,
- Journal of Polymer Science. 58 (2020) 1347–1364. https://doi.org/10.1002/pol.20190261.
- 636 [15] S.M. Al-Salem, P. Lettieri, J. Baeyens, Recycling and recovery routes of plastic solid waste
- 637 (PSW): A review, Waste Management. 29 (2009) 2625–2643.
- https://doi.org/10.1016/j.wasman.2009.06.004.
- 639 [16] J. Ma, P.A. Tominac, H.A. Aguirre-Villegas, O.O. Olafasakin, M.M. Wright, C.H. Benson,
- 640 G.W. Huber, V.M. Zavala, Economic evaluation of infrastructures for thermochemical
- 641 upcycling of post-consumer plastic waste, Green Chemistry. 25 (2023) 1032–1044.
- 642 [17] K. Ragaert, L. Delva, K. Van Geem, Mechanical and chemical recycling of solid plastic
- 643 waste, Waste Management. 69 (2017) 24–58.
- https://doi.org/10.1016/j.wasman.2017.07.044.
- 645 [18] E. Barnard, J.J. Rubio Arias, W. Thielemans, Chemolytic depolymerisation of PET: a
- review, Green Chemistry. 23 (2021) 3765–3789. https://doi.org/10.1039/d1gc00887k.
- 647 [19] A.W. Tricker, A.A. Osibo, Y. Chang, J.X. Kang, A. Ganesan, E. Anglou, F. Boukouvala,
- S. Nair, C.W. Jones, C. Sievers, Stages and Kinetics of Mechanochemical
- Depolymerization of Poly (ethylene terephthalate) with Sodium Hydroxide, ACS Sustain
- 650 Chem Eng. (2022).

- 651 [20] C. Sempels, J. Hoffmann, Circular Economy, Sustainable Innovation Strategy. (2013) 6–9.
- https://doi.org/10.1057/9781137352613.0008.
- 653 [21] I. Nishimura, Strategy for Plastics in a Circular Economy, Seikei-Kakou. 30 (2018) 577–
- 580. https://doi.org/10.4325/seikeikakou.30.577.
- 655 [22] R. Meys, F. Frick, S. Westhues, A. Sternberg, J. Klankermayer, A. Bardow, Towards a
- 656 circular economy for plastic packaging wastes the environmental potential of chemical
- 657 recycling, Resour Conserv Recycl. 162 (2020).
- https://doi.org/10.1016/j.resconrec.2020.105010.
- 659 [23] T. Helmer Pedersen, F. Conti, Improving the circular economy via hydrothermal processing
- of high-density waste plastics, Waste Management. 68 (2017) 24–31.
- https://doi.org/10.1016/j.wasman.2017.06.002.
- 662 [24] S.D. Mancini, M. Zanin, Post Consumer Pet Depolymerization by Acid Hydrolysis,
- 663 Http://Dx.Doi.Org/10.1080/03602550601152945. 46 (2007) 135–144.
- https://doi.org/10.1080/03602550601152945.
- 665 [25] S. Mishra, A.S. Goje, V.S. Zope, Chemical Recycling, Kinetics, and Thermodynamics of
- Poly (Ethylene Terephthalate) (PET) Waste Powder by Nitric Acid Hydrolysis,
- 667 Http://Dx.Doi.Org/10.1081/PRE-120018586. 11 (2017) 79–99.
- https://doi.org/10.1081/PRE-120018586.

- 669 [26] T. Yoshioka, N. Okayama, A. Okuwaki, Kinetics of Hydrolysis of PET Powder in Nitric
- Acid by a Modified Shrinking-Core Model, Ind Eng Chem Res. 37 (1998) 336–340.
- 671 https://doi.org/10.1021/IE970459A.
- 672 [27] A. Palme, A. Peterson, H. de la Motte, H. Theliander, H. Brelid, Development of an efficient
- 673 route for combined recycling of PET and cotton from mixed fabrics, Textiles and Clothing
- 674 Sustainability. 3 (2017). https://doi.org/10.1186/s40689-017-0026-9.
- 675 [28] M. Barth, R. Wei, T. Oeser, J. Then, J. Schmidt, F. Wohlgemuth, W. Zimmermann,
- Enzymatic hydrolysis of polyethylene terephthalate films in an ultrafiltration membrane
- 677 reactor, J Memb Sci. 494 (2015) 182–187. https://doi.org/10.1016/j.memsci.2015.07.030.
- 678 [29] J.A. Schwartz, P.E.A. Acquah, United States Patent (19), 54 (1995).
- 679 [30] R. López-Fonseca, M.P. González-Marcos, J.R. González-Velasco, J.I. Gutiérrez-Ortiz,
- 680 Chemical recycling of PET by alkaline hydrolysis in the presence of quaternary
- phosphonium and ammonium salts as phase transfer catalysts, WIT Transactions on
- Ecology and the Environment. 109 (2008) 511–520. https://doi.org/10.2495/WM080521.
- 683 [31] J.V. Valh, B. Vončina, A. Lobnik, L.F. Zemljič, L. Škodič, S. Vajnhandl, Conversion of
- polyethylene terephthalate to high-quality terephthalic acid by hydrothermal hydrolysis: the
- study of process parameters, Textile Research Journal. 90 (2020) 1446–1461.
- https://doi.org/10.1177/0040517519893714.
- 687 [32] S.D. Mancini, M. Zanin, Optimization of Neutral Hydrolysis Reaction of Post-consumer
- 688 PET for Chemical Recycling, 20 (2004).

- 689 [33] F. Chen, G. Wang, W. Li, F. Yang, Glycolysis of poly(ethylene terephthalate) over Mg-Al
- mixed oxides catalysts derived from hydrotalcites, Ind Eng Chem Res. 52 (2013) 565–571.
- 691 https://doi.org/10.1021/ie302091j.
- 692 [34] Q. Wang, Y. Geng, X. Lu, S. Zhang, First-row transition metal-containing ionic liquids as
- highly active catalysts for the glycolysis of poly(ethylene terephthalate) (PET), ACS Sustain
- 694 Chem Eng. 3 (2015) 340–348. https://doi.org/10.1021/sc5007522.
- 695 [35] Y. Liu, X. Yao, H. Yao, Q. Zhou, J. Xin, X. Lu, S. Zhang, Degradation of poly(ethylene
- terephthalate) catalyzed by metal-free choline-based ionic liquids, Green Chemistry. 22
- 697 (2020) 3122–3131. https://doi.org/10.1039/d0gc00327a.
- 698 [36] B. Allen, G. Breyta, J. Garcia, G. Jones, J. Hedrick, Polyester Digestion: VOLCAT Summit
- on Realizing the IBM Materials Innovation: Polymer Materials, (2018).
- 700 [37] Y. Asakuma, Y. Yamamura, K. Nakagawa, K. Maeda, K. Fukui, Mechanism of
- Depolymerization Reaction of Polyethylene Terephthalate: Experimental and Theoretical
- 702 Studies, J Polym Environ. 19 (2011) 209–216. https://doi.org/10.1007/s10924-010-0263-3.
- 703 [38] M. Han, Depolymerization of PET Bottle via Methanolysis and Hydrolysis, Recycling of
- Polyethylene Terephthalate Bottles. (2019) 85–108. https://doi.org/10.1016/B978-0-12-
- 705 811361-5.00005-5.
- 706 [39] V. Štrukil, Highly Efficient Solid-State Hydrolysis of Waste Polyethylene Terephthalate by
- Mechanochemical Milling and Vapor-Assisted Aging, ChemSusChem. (2020)
- 708 https://doi.org/10.1002/cssc.202002124.

- 709 [40] A.W. Tricker, K.L. Hebisch, M. Buchmann, Y.-H. Liu, M. Rose, E. Stavitski, A.J. Medford,
- 710 M.C. Hatzell, C. Sievers, Mechanocatalytic Ammonia Synthesis over TiN in Transient
- 711 Microenvironments, ACS Energy Lett. 5 (2020) 3362–3367.
- 712 https://doi.org/10.1021/acsenergylett.0c01895.
- 713 [41] J. Lu, S. Borjigin, S. Kumagai, T. Kameda, Y. Saito, T. Yoshioka, Practical dechlorination
- of polyvinyl chloride wastes in NaOH/ethylene glycol using an up-scale ball mill reactor
- and validation by discrete element method simulations, Waste Management. 99 (2019) 31–
- 716 41.
- 717 [42] E. Jung, D. Yim, H. Kim, G.I. Peterson, T. Choi, Depolymerization of poly (α-methyl
- styrene) with ball-mill grinding, Journal of Polymer Science. 61 (2023) 553–560.
- 719 [43] M. Baláž, Z. Bujňáková, M. Achimovičová, M. Tešinský, P. Baláž, Simultaneous
- valorization of polyvinyl chloride and eggshell wastes by a semi-industrial
- mechanochemical approach, Environ Res. 170 (2019) 332–336.
- 722 [44] V.P. Balema, I.Z. Hlova, S.L. Carnahan, M. Seyedi, O. Dolotko, A.J. Rossini, I. Luzinov,
- Depolymerization of polystyrene under ambient conditions, New Journal of Chemistry. 45
- 724 (2021) 2935–2938.
- 725 [45] J. Zhao, Y. Shu, Q. Niu, P. Zhang, Processing Plastic Wastes into Value-Added Carbon
- Adsorbents by Sulfur-Based Solvothermal Synthesis, ACS Sustain Chem Eng. 11 (2023)
- 727 11207–11218. https://doi.org/10.1021/acssuschemeng.3c02049.

- 728 [46] J. Zhao, Q. Niu, J. Zhang, P. Zhang, Core-shell construction of metal@carbon by
- mechanochemically recycling plastic wastes: towards an efficient oxygen evolution
- reaction, Green Chemistry. 25 (2023) 8047–8056. https://doi.org/10.1039/d3gc02695g.
- 731 [47] S. Aydonat, A.H. Hergesell, C.L. Seitzinger, R. Lennarz, Y. Chang, C. Sievers, J. Meisner,
- 732 I. Vollmer, R. Göstl, Leveraging mechanochemistry for sustainable polymer degradation,
- Polymer Journal (Accepted). (2023).
- 734 [48] A. Aguado, L. Martínez, L. Becerra, M. Arieta-araunabeña, S. Arnaiz, A. Asueta, I.
- Robertson, Chemical depolymerisation of PET complex waste: Hydrolysis vs. glycolysis, J
- 736 Mater Cycles Waste Manag. 16 (2014) 201–210. https://doi.org/10.1007/s10163-013-0177-
- 737 y.
- 738 [49] A. Singh, N.A. Rorrer, S.R. Nicholson, E. Erickson, J.S. DesVeaux, A.F.T. Avelino, P.
- Lamers, A. Bhatt, Y. Zhang, G. Avery, Techno-economic, life-cycle, and socioeconomic
- impact analysis of enzymatic recycling of poly (ethylene terephthalate), Joule. 5 (2021)
- 741 2479–2503.
- 742 [50] Aspen Plus, Aspen Technology V12.1 User guide, Inc., Cambridge, MA. (n.d.).
- 743 [51] P.S.E. Ltd., gProms advanced user guide, (2004).
- 744 [52] F. Boukouvala, R. Ramachandran, A. Vanarase, F.J. Muzzio, M.G. Ierapetritou, Computer
- Aided Design and Analysis of Continuous Pharmaceutical Manufacturing Processes, in:
- E.N. Pistikopoulos, M.C. Georgiadis, A.C. Kokossis (Eds.), Computer Aided Chemical

- 747 Engineering, Elsevier, 2011: pp. 216–220. https://doi.org/https://doi.org/10.1016/B978-0-
- 748 444-53711-9.50044-4.
- 749 [53] Z. Wang, C. Ma, A. Shen, A. Berchenko, S.A. Singuefield, S. Nair, Kraft black liquor
- concentration with graphene oxide membranes: Process simulations and technoeconomic
- 751 analysis, J Adv Manuf Process. 3 (2021) e10104–e10104.
- 752 [54] G. Stephanopoulos, G. V Reklaitis, Process systems engineering: From Solvay to modern
- bio- and nanotechnology.. A history of development, successes and prospects for the future,
- 754 Chem Eng Sci. 66 (2011) 4272–4306. https://doi.org/10.1016/j.ces.2011.05.049.
- 755 [55] Y. Luo, E. Selvam, D.G. Vlachos, M. Ierapetritou, Economic and Environmental Benefits
- of Modular Microwave-Assisted Polyethylene Terephthalate Depolymerization, ACS
- 757 Sustain Chem Eng. 11 (2023) 4209–4218. https://doi.org/10.1021/acssuschemeng.2c07203.
- 758 [56] Y. Luo, E. Selvam, D.G. Vlachos, M. Ierapetritou, Economic and Environmental Benefits
- of Modular Microwave-Assisted Polyethylene Terephthalate Depolymerization, ACS
- 760 Sustain Chem Eng. 11 (2023) 4209–4218. https://doi.org/10.1021/acssuschemeng.2c07203.
- 761 [57] B. Hernández, P. Kots, E. Selvam, D.G. Vlachos, M.G. Ierapetritou, Techno-Economic and
- Life Cycle Analyses of Thermochemical Upcycling Technologies of Low-Density
- Polyethylene Waste, ACS Sustain Chem Eng. 11 (2023) 7170–7181.
- https://doi.org/10.1021/acssuschemeng.3c00636.
- 765 [58] T. Uekert, A. Singh, J.S. Des Veaux, T. Ghosh, A. Bhatt, G. Yadav, S. Afzal, J. Walzberg,
- 766 K.M. Knauer, S.R. Nicholson, G.T. Beckham, A.C. Carpenter, Technical, Economic, and

- 767 Environmental Comparison of Closed-Loop Recycling Technologies for Common Plastics,
- 768 ACS Sustain Chem Eng. 11 (2023) 965–978.
- 769 https://doi.org/10.1021/acssuschemeng.2c05497.
- 770 [59] T. Uekert, A. Singh, J.S. DesVeaux, T. Ghosh, A. Bhatt, G. Yadav, S. Afzal, J. Walzberg,
- 771 K.M. Knauer, S.R. Nicholson, Technical, Economic, and Environmental Comparison of
- Closed-Loop Recycling Technologies for Common Plastics, ACS Sustain Chem Eng.
- 773 (2023).
- 774 [60] Altair EDEM 2021.1 Simulation Software, (n.d.).
- 775 [61] X. Bian, G. Wang, H. Wang, S. Wang, W. Lv, Effect of lifters and mill speed on particle
- behaviour, torque, and power consumption of a tumbling ball mill: Experimental study and
- 777 DEM simulation, Miner Eng. 105 (2017) 22–35.
- 778 https://doi.org/https://doi.org/10.1016/j.mineng.2016.12.014.
- 779 [62] W.D. Seider, J.D. Seader, D.R. Lewin, S. Widagdo, Product and process design principles:
- 780 synthesis, Analysis and Evaluation. 4 (2004).
- 781 [63] E. Anglou, Y. Chang, A. Ganesan, S. Nair, C. Sievers, F. Boukouvala, Discrete Element
- 782 Simulation and Economics of Mechanochemical Grinding of Plastic Waste at an Industrial
- Scale, in: Computer Aided Chemical Engineering, Elsevier, 2023: pp. 2405–2410.
- 784 [64] D.A. Longhurst, Economics and methodology of ball mill media maintenance, in: 2010
- 785 IEEE-IAS/PCA 52nd Cement Industry Technical Conference, IEEE, 2010: pp. 1–20.

- 786 [65] C. Swart, J.M. Gaylard, M.M. Bwalya, A Technical and Economic Comparison of Ball Mill
- Limestone Comminution with a Vertical Roller Mill, Mineral Processing and Extractive
- 788 Metallurgy Review. 43 (2022) 275–282.
- 789 [66] Postconsumer PET Recycling Activity in 2018, (n.d.).
- 790 https://doi.org/https://napcor.com/wp-content/uploads/2021/07/Postconsumer-PET-
- 791 Recycling-Activity-in-2018.pdf.
- 792 [67] ICIS Database, (n.d.). https://www.icis.com/subscriber/icb/2017/03/01/10083538/us-
- acetone-faces-prolonged-tightness/#_= (accessed December 5, 2023).
- 794 [68] L. Dessbesell, Z. Yuan, S. Hamilton, M. Leitch, R. Pulkki, C. Xu, Bio-based polymers
- production in a kraft lignin biorefinery: techno-economic assessment, Biofuels, Bioproducts
- 796 and Biorefining. 12 (2018) 239–250.
- 797 [69] V. Pham, M. Holtzapple, M.M. El-Halwagi, Technoeconomic analysis of a lignocellulose-
- 798 to-hydrocarbons process using a carboxylate platform, Integrated Biorefineries: Design,
- 799 Analysis, and Optimization. (2013) 157–192.
- 800 [70] G.E. Brown, R.C. O, Method for recovering terephthalic acid and ethylene glycol from
- polyester materials, (1974).
- 802 [71] W. Li, B. Van der Bruggen, P. Luis, Integration of reverse osmosis and membrane
- 803 crystallization for sodium sulphate recovery, Chemical Engineering and Processing:
- Process Intensification. 85 (2014) 57–68. https://doi.org/10.1016/J.CEP.2014.08.003.

805 P. Europe, Plastics—The Facts 2016, An Analysis of European Plastics Production, 806 Demand and Waste Data. (2016) 1-38. 807 I.M. Steensgaard, K. Syberg, S. Rist, N.B. Hartmann, A. Boldrin, S.F. Hansen, From macroto microplastics-Analysis of EU regulation along the life cycle of plastic bags, 808 809 Environmental Pollution. 224 (2017) 289–299. 810 Vermont Government, Department of Environmental Conservation, [74] (n.d.). 811 https://dec.vermont.gov/waste-management/solid/materials-mgmt/what-happens-my-stuff 812 (accessed June 14, 2023). 813